5-AXIS PARALLEL KINEMATIC ROBOT

A Final Year Project Report

Presented to

SCHOOL OF MECHANICAL & MANUFACTURING ENGINEERING

Department of Mechanical Engineering

NUST

ISLAMABAD, PAKISTAN

In Partial Fulfillment
of the Requirements for the Degree of
Bachelors of Mechanical Engineering

By
Ahmed Ali Siddiqui
Muhammad Ahsan Saleem
Muhammad Hamza
Somaan Shakeel

June 2024

EXAMINATION COMMITTEE

We hereby recommend that the final year project report prepared under our supervision by:

Ahmed Ali Siddiqui	331589
Muhammad Ahsan Saleem	333106
Muhammad Hamza	338848
Somaan Shakeel	331275

Titled: "5-Axis Parallel Kinematic Robot" be accepted in partial fulfillment of the requirements for the award of BACHELOR OF MECHANICAL ENGINEERING degree with grade ___

Supervisor: Dr. Khawaja Fahad Iqbal, Assistant Professor, SMME - NUST	Dated: 19/9/2024
Committee Member: Name, Title (faculty rank) Affiliation	Dated:
Committee Member: Name, Title (faculty rank) Affiliation	Dated:

(Head of Department)

19/9/2024
(Date)

COUNTERSIGNED

Dated: 19-9-24

(Dean / Principal)

ABSTRACT

Our project aims at the design and development of a 5-DOF Parallel Kinematic Robot, that will be easily programmable by an operator.

The economic strength of any country is measured by the quality and speed of its production. Due to technological advancements, industries are utilizing robots to perform tasks that human labor is unable to perform at a fast rate. Developed countries such as China, South Korea, Japan, USA, UK, France, and Russia are using industrial robots for most of their manufacturing processes.

Unfortunately, in Pakistan, the use of industrial robots is very minimal. It is the need of the hour to speed up our production rates using the help of such robots.

The goal of developing this robot is to provide a method of building an industrial robot, that can be replicated by other companies in Pakistan, so that our industries have the option of buying locally built robots, rather than having to import at expensive rates.

ACKNOWLEDGMENTS

We extend our sincere gratitude to all those who played a pivotal role in making the completion of this report possible. Our heartfelt thanks go out to our esteemed advisor, Dr. Khawaja Fahad Iqbal whose expertise and encouragement were invaluable in shaping the direction of our work. A special acknowledgment is due to our dedicated final year project coordinator Dr. Rehan Zahid whose insightful suggestions and constant encouragement helped us effectively coordinate our project, ensuring its successful execution. We are grateful for his mentorship and commitment to our academic growth. We must also express our gratitude to Dr. Jawad Aslam who was our co-supervisor for a short duration before leaving the university. His advice on technical matters along with providing partial funding was one of the crucial parts of our project.

ORIGINALITY REPORT

5-Axis

ORIGINALITY REPORT

6%	4%	4%	3%
SIMILARITY INDEX	INTERNET SOURCES	PUBLICATIONS	STUDENT PAPERS

PRIMARY SOURCES

1	www.coursehero.com Internet Source	1%
2	Submitted to Staffordshire University Student Paper	1%
3	www2.gov.bc.ca Internet Source	<1%
4	"New Advances in Mechanisms, Transmissions and Applications", Springer Science and Business Media LLC, 2023 Publication	<1%
5	Submitted to The Robert Gordon University Student Paper	<1%
6	"Advances in Industrial Machines and Mechanisms", Springer Science and Business Media LLC, 2021 Publication	<1%
7	Sachin Kansal, Sudipto Mukherjee. "Vision-based kinematic analysis of the Delta robot for object catching", Robotica, 2021 Publication	<1%

TABLE OF CONTENTS

LIST OF TABLES

LIST OF FIGURES

ABBREVIATIONS

STM	Synchronous Transport Module

CHAPTER 1: INTRODUCTION

It is common knowledge that there is a lack of manufacturing in Pakistan. Even where manufacturing does take place, there is a lack of industrial robots that can improve the efficiency of production. Industrial robots are a necessity for large scale manufacturing in today's day and age.

Figure 1: An Assembly Line in Lahore [1]

Leading economies such as China and the US are heavily using Industrial robots to increase their manufacturing capacity. In 2020, China accounted for more than half of the world's industrial robot installations. [2]

The reason for this is that industrial robots produce high quality work with fewer mistakes. Their rate of production is higher and can work 24/7 unlike human workers.

In Pakistan, there is little to no use of Industrial robots, and one of the reasons is the lack of locally manufactured robots. Foreign companies such as Yaskawa, ABB etc. produce robots that are too expensive for a Pakistani company.

To tackle this problem, we have decided to build a prototype for an Industrial robot that can be used as a proof of concept for others to build upon.

Furthermore, there are two broad types of robotic manipulators in terms of structure, namely serial and parallel robots. We have decided to build a parallel robot due to its higher precision and higher stiffness. This has been elaborated in detail in the literature review section.

In addition to this, we wish to make this robot as flexible as possible such that even very complex tasks that require higher degrees of freedom can also be performed. Therefore, we have decided to build a 5 DOF robot. Moreover, we will be designing the end-effector to be suitable for welding so that we can design with a specific application in mind.

We will be taking our inspiration from a Swedish company called Cognibotics that have been developing a 5 DOF parallel robot as in the image below:

Figure 2: Cognibotics 5 DOF Parallel Robot [3]

1.1 Deliverables

- A working prototype of a 5 DOF Parallel Robot
- CAD models of the entire robot and all its parts
- Finite Element Analysis of all its parts
- Simulation of the entire robot in a physics engine

CHAPTER 2: LITERATURE REVIEW

2.1 Industrial Robots:

Industrial robots play a vital role in the manufacturing industry. These robots are employed in a range of area such as payloader, welding, painting, packing, assembling, and other critical areas.

According to a report by the International Federation of Robotics, in 2010, China had a robot density of 23 Industrial robots per 10,000 employees. As the graph indicates, in just 10 years, this number has risen to 243 Industrial robots per 10,000 employees. [2]

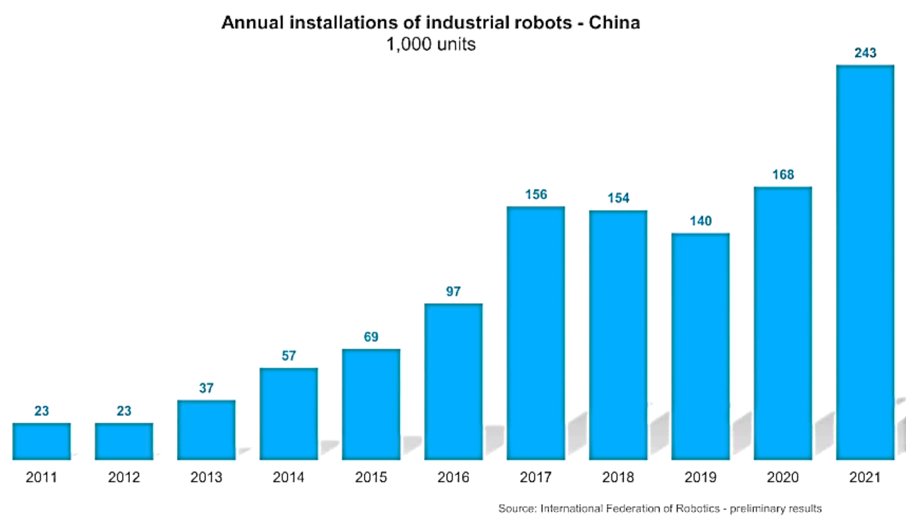

Figure 3: Annual installations of Industrial Robots in China [2]

In 2021, China accounted for half of the world's robot installations. [4] Besides China, we can see that all the top manufacturing countries like the South Korea, Singapore, USA, Germany, Japan all have a high robot density. It's obvious that for a country to succeed in manufacturing high quality goods in high amounts, it is necessary to incorporate industrial robots into its factories.

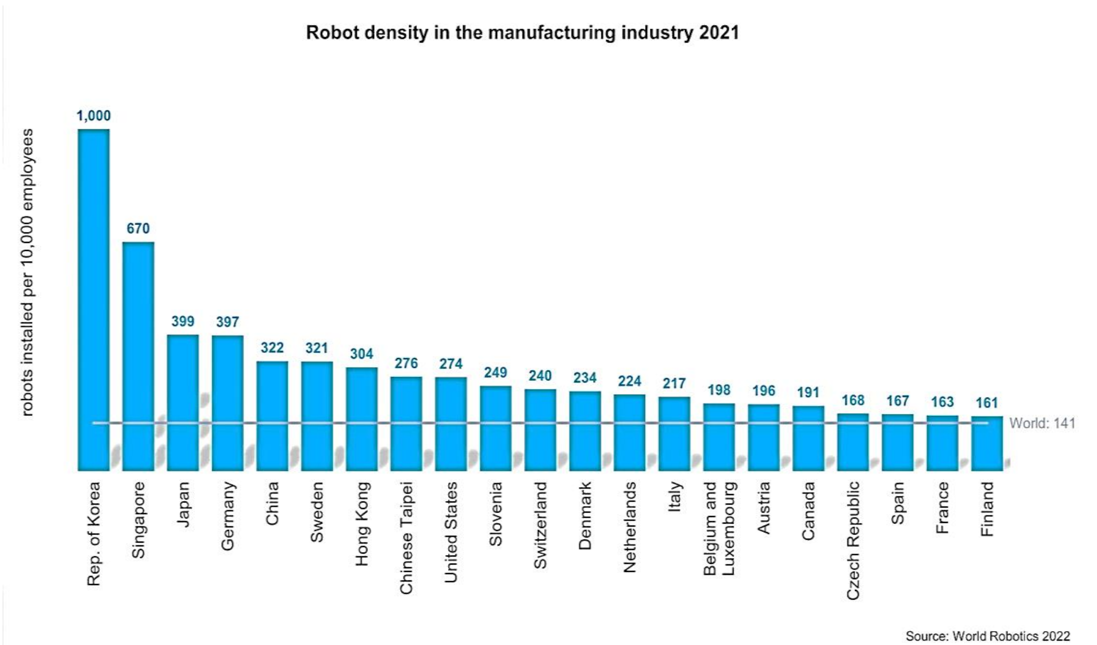

Figure 4: Global Robot Density [4]

2.2 Industrial Robots in Pakistan

Although the manufacturing in Pakistan is already low, for the manufacturing that does take place, there is little to no use of Industrial robots. One of the reasons is the lack of local companies producing quality robots that can be used to reliably perform critical tasks in the factory. Importing robots from companies such as Yaskawa, ABB and others is extremely expensive, especially with our depreciating currency. An Industrial Robot can cost anywhere from $25,000 to $400,000 which translates to 70 lacs to 11 Crore in Pakistani rupees. [5] This helps us clear our goal that we must design, manufacture, and optimize a cheap yet reliable industrial robot.

2.3 Serial vs. Parallel Robots

A Serial robot is an Open Chain Robot. It usually has motors on each link, increasing the mass that must be moved, thereby increasing its inertia. This prevents the robot from achieving high acceleration.

Furthermore, serial robots have a low load-to-mass ratio, which means that a serial robot's own mass needs to be quite high, for it to lift a high load. [6]

But the most important aspect of serial robots is the fact that their errors are compound. For example, if the motors of a serial manipulator are off by a tiny amount, those errors will add up and the resultant error will be large, making it difficult to achieve very high accuracy.

Parallel Robots, on the other hand, have a closed chain, and they don't have motors on their forearms, lowering the mass that must be moved. This low inertia allows for higher acceleration. [7] For the same reason, they have a high load-to-mass ratio. But the most important advantage of such a robot is that the errors don't compound because the links are not attached one-after-the-other as they are in Serial Robots.

But under the category of Parallel robots, there are many further types.

One of the most common types of parallel robots is a delta robot with Revolute joints. This is a 3 DOF Delta-type robot with 3 motors at its base that control where the end-effector moves.

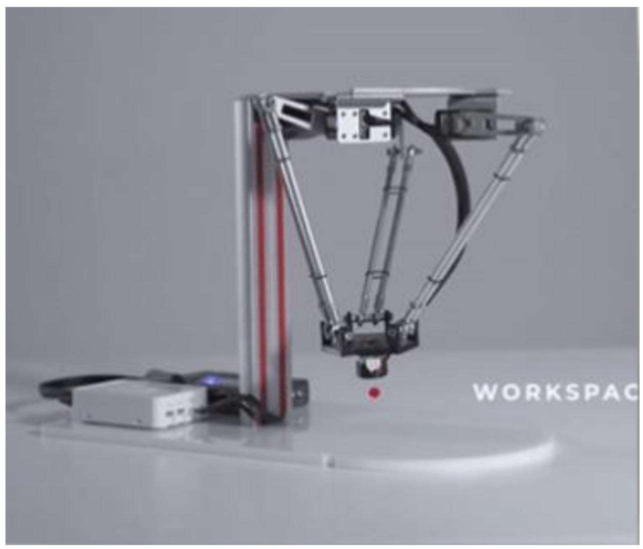

Figure 5: Delta Robot with 3 Revolute Joints

Another variation is the use of linear actuators at the base, instead of Revolute joints. This also results in a similar workspace, as shown in pink below:

Figure 6: Delta Robot with 3 Linear Actuator at an angle

Another popular variation is with linear actuators aligned vertically. It's one of the most popular designs utilized by parallel 3D printers. The problem with this design is that one can't pass a conveyor belt through them as the actuators are in a triangular shape.

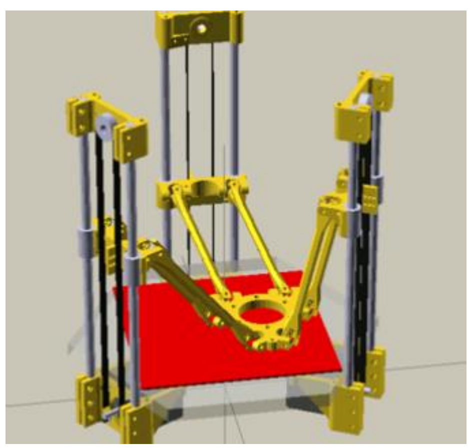

Figure 7: Delta Robot with Vertically Aligned Actuators

We gained our inspiration from a Swedish Company called Cognibotics. The design has three linear actuators, on top, left and right, to move the end effector in 3D space.

Furthermore, it is very simple to mount over a conveyor belt and it has a larger workspace for the same lengths of linear actuators, compared to the other designs.

CHAPTER 3: METHODOLOGY

We started off by performing extensive research on the different components, actuators, microcontrollers, supporting structures that would be optimum for our project while keeping in mind the cost and availability within Pakistan.

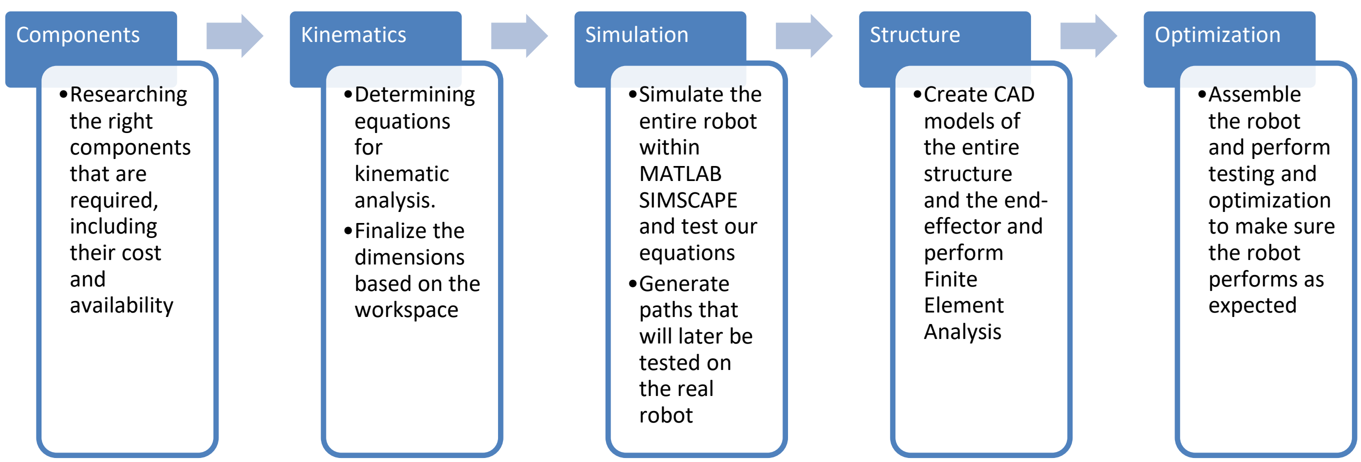

3.1 Linear Actuators

Our project involves 5 degrees of freedom where the end-effector will have the ability to translate in 3D space while also being able to rotate along two further axes. To accomplish this, we need 3 main linear actuators that will move the entire end-effector within 3D space.

We settled on the 1 m Linear Actuators by Intellitek which were available to us within SMME. These actuators had the ability to provide sufficient torque and speed to move the end-effector according to our requirements, as described below:

Specification	Units	14201 24.0 V
Supply Voltage	VDC	24.0
Continuous Torque	oz-in	10
	Nm	0.0706
Speed @ Cont. Torque	RPM	3330
Current @ Cont. Torque	Amps (A)	1.79
Continuous Output Power	Watts (W)	25
Motor Constant	oz-in/sqrt W	4.5
	Nm/sqrt W	0.032
Torque Constant	oz-in/A	7.44
	Nm/A	0.053
Voltage Constant	V/krpm	5.50
	V/rad/s	0.053
Terminal Resistance	Ohms	2.79
Inductance	mH	2.54
No-Load Current	Amps (A)	0.26
No-Load Speed	RPM	4150
Peak Current	Amps (A)	8.60
Peak Torque	oz-in	62.1
	Nm	0.4384
Coulomb Friction Torque	oz-in	1.2
	Nm	0.0085
Viscous Damping Factor	oz-in/krpm	0.17
	Nm s/rad	1.14E-5
Electrical Time Constant	ms	0.91
Mechanical Time Constant	ms	11
Thermal Time Constant	min	22
Thermal Resistance	Celsius/W	9.9
Max. Winding Temperature	Celsius	155
Rotor Inertia	oz-in-sec2	0.0016
	kg-m2	1.13E-5
Weight (Mass)	oz	20.8
	g	589.7

Figure 8: Motor Characteristics

Continuous Torque of Motor is 0.0706 Nm, however there is a gear box attached to the motor as shown below:

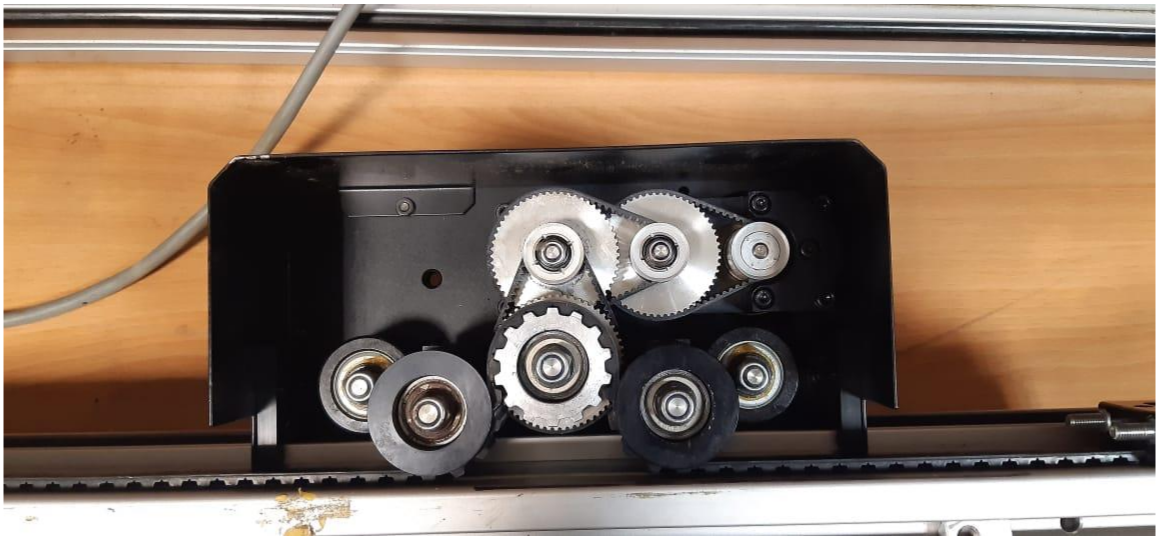

Figure 9: Gearbox of the Linear Actuators

After taking this gearbox into account, the continuous Torque of Actuator comes out to be 0.63546 Nm. By using the radius of the final pulley, we calculated that the force that can be exerted by this actuator is 28.242 N. Since three of these actuators are being used, they will have a combined capacity of around 84 N which means that an end-effector of 8 kg can easily be moved around continuously.

Figure 10: Intelletik Actuators

3.2 Microcontroller

As for the brains of the robot, we initially attempted to use an Arduino Uno, however it did not provide us with enough Timers that we could use to read our encoders. We did our research on Arduino Mega as well, but that also did not have the ability to read three or more encoders at once.

Finally, we settled on the STM32 F407 Discovery Board. This microcontroller features a 32-bit Arm Cortex – M4 with FPU core, 1-Mbyte Flash memory and 192-Kbyte RAM. It has 11 timers, include “Advanced Timers” that have the ability to directly read encoders through a special “Encoder Mode”.

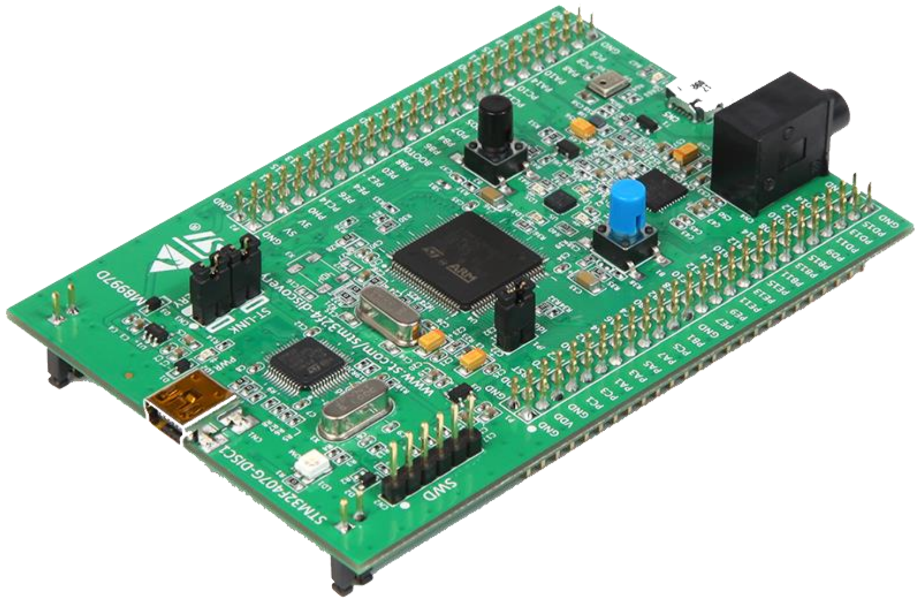

Figure 11: STM32 F407 Discovery Board

3.3 Further Two Linear Actuators for Final Two Axes

To rotate the end-effector at further two angles, we require two more actuators. Because we will to keep as little weight as possible on the end-effector itself, we won't be attaching motors on the effector to rotate the nib, instead, we'll use two more linear actuators to "push" and "pull" upon the nib, causing it to rotate at our desired angle.

The following actuators were easily available and affordable for us to use in this project.

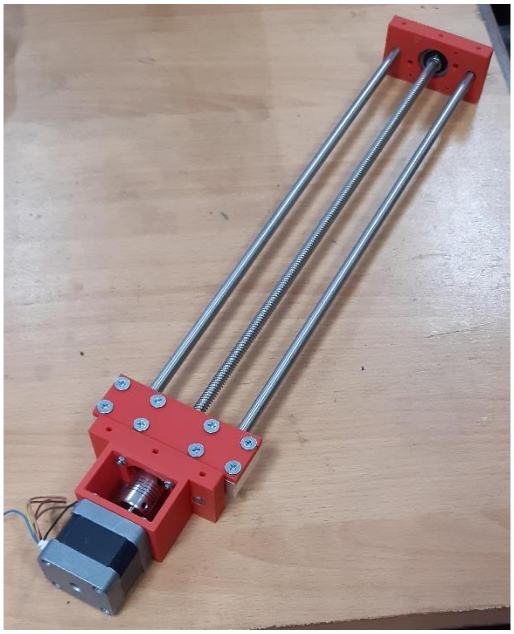

Figure 12: Linear actuator for the final two axes

Figure 13: How the actuator is attached to the main actuator

These linear actuators have the following specifications:

- 12V Rated Voltage
- 1.2A Current Rating
- 1.8 deg Step Angle.
- 4 Phases
- 1.54 inches Motor Length

- 8 inch lead, 4-wire
- 200 steps per revolution
- Operating Temp.: -10 to 40 °C
- Unipolar Holding Torque: 22.2 oz-in

These actuators were bought off the shelf as they were enough to provide the minimal torque that we required.

3.4 Motor Drivers

For our three main linear actuators that will move the end-effector in 3D space, the current requirement is very high. The motor can draw a peak current of 8.6 Amps. Therefore, we decided to use a high-current motor bridge called “IBT-2”

Figure 14: IBT-2 Motor Driver

This motor driver can allow for the withdrawal of up to 43 Amps, which means there is a factor of safety of 5 within our system.

As for the two stepper motors in the lower actuators, the motor driver used was the DRV8825. This was the most easily available motor driver and had the capability to work at up to 2A when a heat shield is attached to it, therefore it was sufficient for the Nema 17 motors.

Figure 15: DRV8825 Motor Driver

3.5 Forward Kinematics – Vector Loop Equations

To move the end-effector to a desired location, it is necessary to first perform an extensive kinematic analysis on the robot and determine the equations that relate the position of the end-effector to the position of the 5 actuators:

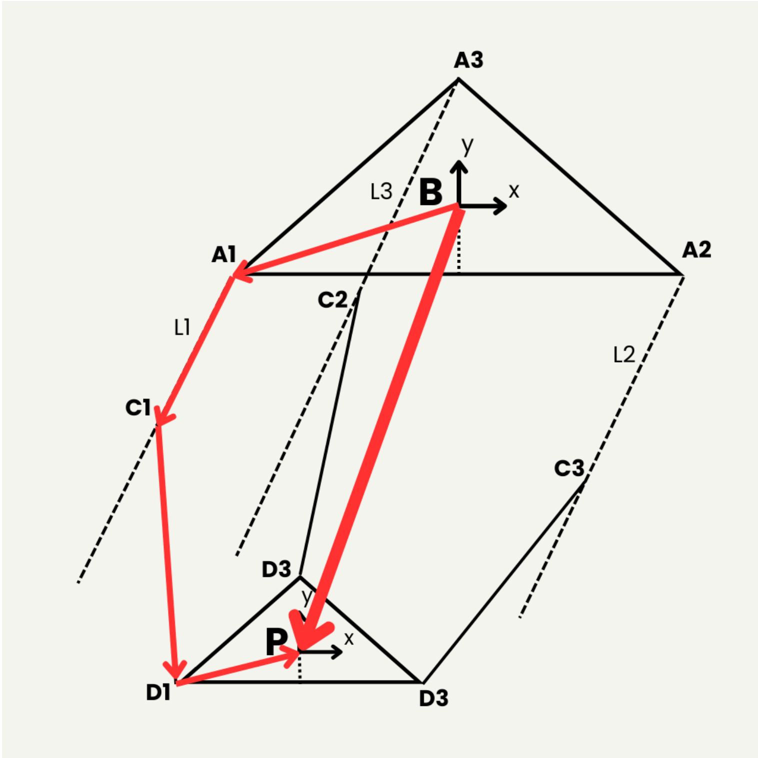

Figure 16: Vector Loop Diagram

The frame B in the image above represents the Base frame from which everything will be referenced. The Frame P represents the frame of the end-effector. Note that for now, this doesn't include the nib that will rotate. For now, it is just the 3D motion of the end-effector that is being analyzed. The rotation of the nib will be taken into account later.

To find the equations for forward, a lot of help was taken from the internet publication by R.L. Williams II. [8]

Using vector loop equations, we can determine for the left actuator that:

$$\overrightarrow{BA_1} + \overrightarrow{A_1C_1} + \overrightarrow{C_1D_1} = \overrightarrow{BP} + \overrightarrow{PD_1}$$

Where $\overrightarrow{BP} = \begin{bmatrix} x \\ y \\ z \end{bmatrix}$ (Position of frame P w.r.t Frame B)

$$\overrightarrow{C_1D_1} = \overrightarrow{BP} + \overrightarrow{PD_1} - \overrightarrow{BA_1} - \overrightarrow{A_1C_1}$$

$$\overrightarrow{C_1D_1} = \begin{bmatrix} x \\ y \\ z \end{bmatrix} + \begin{bmatrix} \frac{-s_p}{2} \\ -w_p \\ 0 \end{bmatrix} - \begin{bmatrix} \frac{-s_B}{2} \\ -w_B \\ 0 \end{bmatrix} - \begin{bmatrix} 0 \\ 0 \\ L_1 \end{bmatrix}$$

$$\overrightarrow{C_1D_1} = \begin{bmatrix} x - \frac{s_p}{2} - \frac{s_B}{2} \\ y - w_p - w_B \\ z - L_1 \end{bmatrix} \rightarrow \overrightarrow{C_1D_1} = \begin{bmatrix} x + a \\ y + b \\ z - L_1 \end{bmatrix}$$

Where:

$$a = -\frac{s_p}{2} - \frac{s_B}{2}$$

$$b = -w_p - w_B$$

Furthermore, we know the magnitude of $\overrightarrow{C_1D_1}$:

$$l_b{}^2 = \left|\overrightarrow{C_1D_1}\right| = (x + a)^2 + (y + b)^2 + (z - L_1)^2$$

$$x^2 + y^2 + z^2 + a^2 + b^2 + L_1{}^2 + 2ax + 2yb - 2zL_1 = l_b{}^2$$

Similarly For Right Actuator:

$$x^2 + y^2 + z^2 + a^2 + b^2 + L_2{}^2 - 2ax + 2yb - 2zL_2 = l_b{}^2$$

For Top Actuator:

$$\overrightarrow{C_3D_3} = \overrightarrow{BP} + \overrightarrow{PD_3} - \overrightarrow{BA_3} - \overrightarrow{A_3C_3}$$

$$\overrightarrow{C_1D_1} = \begin{bmatrix} x \\ y \\ z \end{bmatrix} + \begin{bmatrix} 0 \\ h - w_p \\ 0 \end{bmatrix} - \begin{bmatrix} 0 \\ H - w_B \\ 0 \end{bmatrix} - \begin{bmatrix} 0 \\ 0 \\ L_3 \end{bmatrix}$$

$$\overrightarrow{C_1D_1} = \begin{bmatrix} x \\ y + h - w_p + H - w_B \\ z - L_3 \end{bmatrix} \rightarrow \overrightarrow{C_1D_1} = \begin{bmatrix} x \\ y + c \\ z - L_3 \end{bmatrix}$$

Where,

$$c = h - w_p + H - w_B$$

Once again, we know the length of the top link:

$${l_t}^2 = \left|\overrightarrow{C_3D_3}\right| = (x)^2 + (y + c)^2 + (z - L_3)^2$$

$$x^2 + y^2 + z^2 + c^2 + {L_3}^2 + 2yc - 2zL_3 = {l_t}^2$$

The three equations:

$$x^2 + y^2 + z^2 + a^2 + b^2 + {L_1}^2 + 2ax + 2yb - 2zL_1 - {l_b}^2 = 0 - - - (1)$$

$$x^2 + y^2 + z^2 + a^2 + b^2 + {L_2}^2 - 2ax + 2yb - 2zL_2 - {l_b}^2 = 0 - - - (2)$$

$$x^2 + y^2 + z^2 + c^2 + {L_3}^2 + 2yc - 2zL_3 - {l_t}^2 = 0 - - - (3)$$

Subtract 2 from 1:

$${L_1}^2 + 2ax - 2zL_1 - \left({L_2}^2 - 2ax + 2yb - 2zL_2\right) = 0$$

$${L_1}^2 - {L_2}^2 + 4ax - 2zL_1 + 2zL_2 = 0$$

$$4ax = 2zL_1 - 2zL_2 - {L_1}^2 + {L_2}^2$$

$$x = \frac{2z(L_1 - \mathrm{L}_2)}{4a} + \frac{{L_2}^2 - {L_1}^2}{4a}$$

$$x = \frac{z(L_1 - \mathrm{L}_2)}{2a} + \frac{{L_2}^2 - {L_1}^2}{4a}$$

$$x = dz + e - - - (4)$$

Where:

$$d = \frac{(L_1 - \mathrm{L}_2)}{2a}, \qquad e = \frac{{L_2}^2 - {L_1}^2}{4a}$$

Subtract equation 3 from 1 and substitute 4:

$$c^2 + {L_3}^2 + 2yc - 2zL_3 - {l_t}^2 - (a^2 + b^2 + {L_1}^2 + 2a(dz + e) + 2yb - 2zL_1 - {l_b}^2) = 0$$

$$c^2 + {L_3}^2 + 2yc - 2zL_3 - {l_t}^2 - a^2 - b^2 - {L_1}^2 - 2adz - 2ae - 2yb + 2zL_1 + {l_b}^2 = 0$$

$$2yb - 2yc = c^2 + {L_3}^2 - 2zL_3 - {l_t}^2 - a^2 - b^2 - {L_1}^2 - 2adz - 2ae + 2zL_1 + {l_b}^2$$

$$2y(b - c) = 2z(L_1 - ad - L_3) + c^2 + {L_3}^2 - {l_t}^2 - a^2 - b^2 - {L_1}^2 - 2ae + {l_b}^2$$

$$y = \frac{2z(L_1 - ad - L_3)}{2(b - c)} + \frac{c^2 + {L_3}^2 - {l_t}^2 - a^2 - b^2 - {L_1}^2 - 2ae + {l_b}^2}{2(b - c)}$$

$$y = \frac{z(L_1 - ad - L_3)}{(b - c)} + \frac{c^2 + {L_3}^2 - {l_t}^2 - a^2 - b^2 - {L_1}^2 - 2ae + {l_b}^2}{2(b - c)}$$

$$y = Dz + E - - - (5)$$

Where:

$$D = \frac{(L_1 - ad - L_3)}{(b-c)}, \qquad E = \frac{c^2 + {L_3}^2 - {l_t}^2 - a^2 - b^2 - {L_1}^2 - 2ae + {l_b}^2}{2(b-c)}$$

Substitute eq (4) and (5) in eq (3):

$$(dz+e)^2 + (Dz+E)^2 + z^2 + c^2 + 2c(Dz+E) - 2zL_3 + {L_3}^2 - {l_t}^2 = 0$$

$$(dz)^2 + (e)^2 + 2dez + (Dz)^2 + (E)^2 + 2DEz + z^2 + c^2 + 2cDz + 2cE - 2zL_3 + {L_3}^2 - {l_t}^2 = 0$$

$$\left(d^2 + D^2 + 1\right)z^2 + 2z(de + cD + DE - L_3) + (E)^2 + (e)^2 + c^2 + 2cE + {L_3}^2 - {l_t}^2 = 0$$

The above equation is similar to a quadratic equation:

$$(M)z^2 + 2z(N) + O = 0$$

Where:

$$M = d^2 + D^2 + 1, \qquad N = de + cD + DE - L_3,$$

$$O = (E)^2 + (e)^2 + c^2 + 2cE + {L_3}^2 - {l_t}^2$$

$$z_{1,2} = \frac{-N \mp \sqrt{N^2 - 4MO}}{2M}$$

$$x_{1,2} = f\left(z_{1,2}\right) = dz_{1,2} + e$$

$$y_{1,2} = g\left(z_{1,2}\right) = Dz_{1,2} + E$$

This is how the position of the end-effector will be determined by the positions of the linear actuators.

Now for the forward kinematics of the nib, we will perform a similar analysis. This time we will find the position of the end of the nib from the center of the upper part of the end-effector (the point whose location we can determine using the equations derived above).

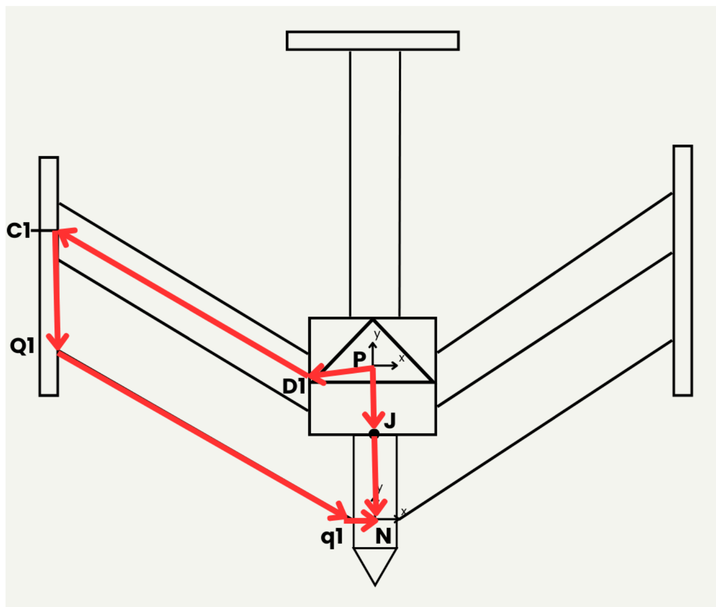

Figure 17: Vector Loop Diagram for the Nib

Now the vector loop equation is as follows:

$$s\overrightarrow{PJ} + \overrightarrow{JN} = \overrightarrow{PD_1} + \overrightarrow{D_1C_1} + \overrightarrow{C_1Q_1} + \overrightarrow{\boldsymbol{Q_1q_1}} + \overrightarrow{q_1N} \ \ , \text{ where } \overrightarrow{JN} = \begin{bmatrix} x_n \\ y_n \\ z_n \end{bmatrix}$$

Given $\overrightarrow{JN}$, we can find $\overrightarrow{\boldsymbol{Q_1 q_1}}$ and its magnitude, which would then give us the position of the lower actuators. For the left actuator:

$$\overrightarrow{PD_1} + \overrightarrow{D_1C_1} + \overrightarrow{C_1Q_1} + \overrightarrow{Q_1q_1} + \overrightarrow{q_1N} = \overrightarrow{PJ} + \overrightarrow{JN}$$

$$\begin{bmatrix} 0 \\ w_p - h \\ 0 \end{bmatrix} + \begin{bmatrix} x_n \\ y_n \\ z_n \end{bmatrix} = \begin{bmatrix} \frac{-s_p}{2} \\ -w_p \\ 0 \end{bmatrix} - \begin{bmatrix} x + a \\ y + b \\ z - L_1 \end{bmatrix} + \begin{bmatrix} 0 \\ -d_q \\ 0 \end{bmatrix} + \overrightarrow{Q_1q_1} + \begin{bmatrix} \frac{w_n}{2} \\ 0 \\ 0 \end{bmatrix}$$

$$\overrightarrow{Q_1q_1} = \begin{bmatrix} x_n \\ y_n - w_p - h \\ z_n \end{bmatrix} - \begin{bmatrix} -\frac{s_p}{2} \\ -w_p \\ 0 \end{bmatrix} + \begin{bmatrix} x + a \\ y + b \\ z - L_1 \end{bmatrix} - \begin{bmatrix} 0 \\ -d_q \\ 0 \end{bmatrix} - \begin{bmatrix} \frac{w_n}{2} \\ 0 \\ 0 \end{bmatrix}$$

$$\overrightarrow{Q_1q_1} = \begin{bmatrix} x_n + \frac{s_p}{2} + x + a - \frac{w_n}{2} \\ y_n - w_p - h + w_p + y + b + d_q \\ z_n + z - L_1 \end{bmatrix}$$

$$\overrightarrow{Q_1q_1} = \begin{bmatrix} x_n + \frac{s_p}{2} + x + a - \frac{w_n}{2} \\ y_n - h + y + b + d_q \\ z_n + z - L_1 \end{bmatrix}$$

But x_n, y_n, z_n are not independent:

$$d_n^{\,2} = x_n^{\,2} + y_n^{\,2} + z_n^{\,2}$$

$$y_n = -\sqrt{d_n^{\,2} - x_n^{\,2} - z_n^{\,2}}$$

It is negative because it will always be below the block. The only two inputs are x_n and z_n and y_n that will depend on the height of the nib. This is how we can find the position of the nib by using the positions of the lower actuators.

3.6 Inverse Kinematics

We need to find the equations that would allow us to find the appropriate location of the linear actuator given the position of the end-effector. This is quite simpler as compared to the forward kinematic equations. Because we know the position of the end-effector, we already know the x, y, and z coordinate of frame P w.r.t frame B. Using the three equations we derived for each of the three actuators above, we can simply place the values of x, y and z back into those equations and we can find the values of L1, L2 and L3.

The three equations derived before:

$$L_1^{\,2} + 2zL_1 + C_1 = 0$$

$$L_2^{\,2} + 2zL_2 + C_2 = 0$$

$$L_3^{\,2} + 2zL_3 + C_3 = 0$$

Where:

$$C_1 = x^2 + y^2 + z^2 + a^2 + b^2 + 2ax + 2yb - l_b^{\,2}$$

$$C_2 = x^2 + y^2 + z^2 + a^2 + b^2 - 2ax + 2yb - {l_b}^2$$

$$C_3 = x^2 + y^2 + z^2 + c^2 + 2yc - {l_t}^2$$

$$L_i = \frac{-(-2z) \mp \sqrt{(-2z)^2 - 4C_i}}{2(1)}$$

$$L_i = \frac{2(z \mp \sqrt{z^2 - C_i})}{2(1)}$$

$$L_i = z \mp \sqrt{z^2 - C_i}, \qquad i = 1, 2, 3$$

All three equations are separate from each other. L1, L2 and L3 can be easily calculated separately as shown above.

3.7 Velocity Analysis - Jacobian

To fully understand our robot, we need to perform a velocity analysis i.e. understand how the velocity of the end-effector relate to the velocity of the actuators. We will use the same equations for position analysis derived above and differentiate them.

Differentiate eqs. (1), (2) and (3)

$$2x\dot{x} + 2y\dot{y} + 2z\dot{z} + 2a\dot{x} + 2b\dot{y} - 2z\dot{L}_1 - 2L_1\dot{z} + 2L_1\dot{L}_1 = 0$$

$$2x\dot{x} + 2a\dot{x} + 2y\dot{y} + 2b\dot{y} + 2z\dot{z} - 2L_1\dot{z} - 2z\dot{L}_1 + 2L_1\dot{L}_1 = 0$$

$$2\dot{x}(x + a) + 2\dot{y}(y + b) + 2\dot{z}(z - L_1) = 2\dot{L}_1(z - L_1)$$

$$\dot{x}(x + a) + \dot{y}(y + b) + \dot{z}(z - L_1) = \dot{L}_1(z - L_1) - - - (1)$$

$$\dot{x}(x - a) + \dot{y}(y + b) + \dot{z}(z - L_2) = \dot{L}_2(z - L_2) - - - (2)$$

$$2x\dot{x} + 2y\dot{y} + 2z\dot{z} + 2c\dot{y} - 2z\dot{L}_3 - 2L_3\dot{z} + 2L_3\dot{L}_3 = 0$$

$$x\dot{x} + \dot{y}(y + c) + \dot{z}(z - L_3) = \dot{L}_3(z - L_3)$$

$$[A]\{\dot{X}\} = [B]\{\dot{L}\}$$

$$\begin{bmatrix} x+a & y+b & z-L_1 \\ x-a & y+b & z-L_2 \\ x & y+c & z-L_3 \end{bmatrix} \begin{bmatrix} \dot{x} \\ \dot{y} \\ \dot{z} \end{bmatrix} = \begin{bmatrix} z-L_1 & 0 & 0 \\ 0 & z-L_2 & 0 \\ 0 & 0 & z-L_3 \end{bmatrix} \begin{bmatrix} \dot{L}_1 \\ \dot{L}_2 \\ \dot{L}_3 \end{bmatrix}$$

Forward Velocity Solution:

$$[\dot{X}] = [A]^{-1}[B][\dot{L}]$$

Inverse Velocity Solution:

$$[\dot{L}] = [B]^{-1}[A][\dot{X}]$$

$$\begin{bmatrix} \dot{L}_1 \\ \dot{L}_2 \\ \dot{L}_3 \end{bmatrix} = \begin{bmatrix} \frac{x+a}{z-L_1} & \frac{y+b}{z-L_1} & 1 \\ \frac{x-a}{z-L_2} & \frac{y+b}{z-L_2} & 1 \\ \frac{x}{z-L_3} & \frac{y+c}{z-L_3} & 1 \end{bmatrix} \begin{bmatrix} \dot{x} \\ \dot{y} \\ \dot{z} \end{bmatrix}$$

3.8 Workspace Calculations

To determine the appropriate dimensions of our robot, we first need to finalize a workspace that we want our robot to move in. Once the workspace is finalized, we need to work backwards to see what dimensions of the outer structure would allow us to achieve that workspace.

To accomplish this task, we created a MATLAB live script that allowed us to visualize the workspace of our robot:

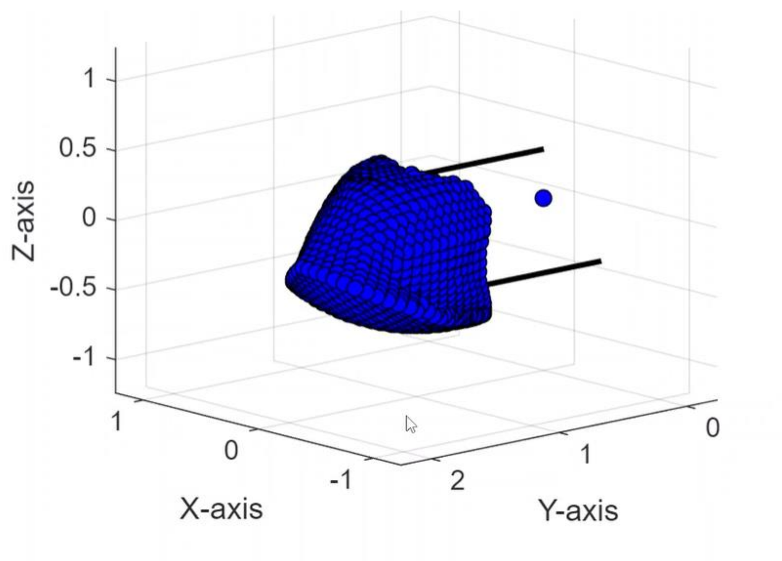

Figure 18: Workspace visualization of our robot

We defined a workspace of 600mm x 500mm x 500mm that we want our robot to move it. That is shown on the simulation below:

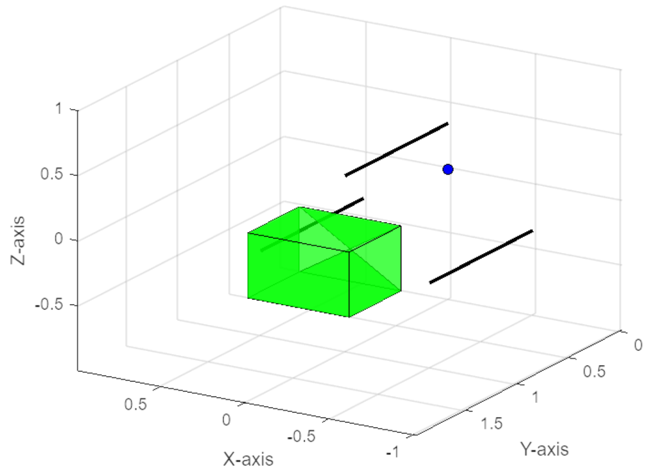

Figure 19: Our desired Workspace

Now to achieve this workspace, we used sliders in the MATLAB workspace to vary the parameters of the robot to fit the workspace around this robot.

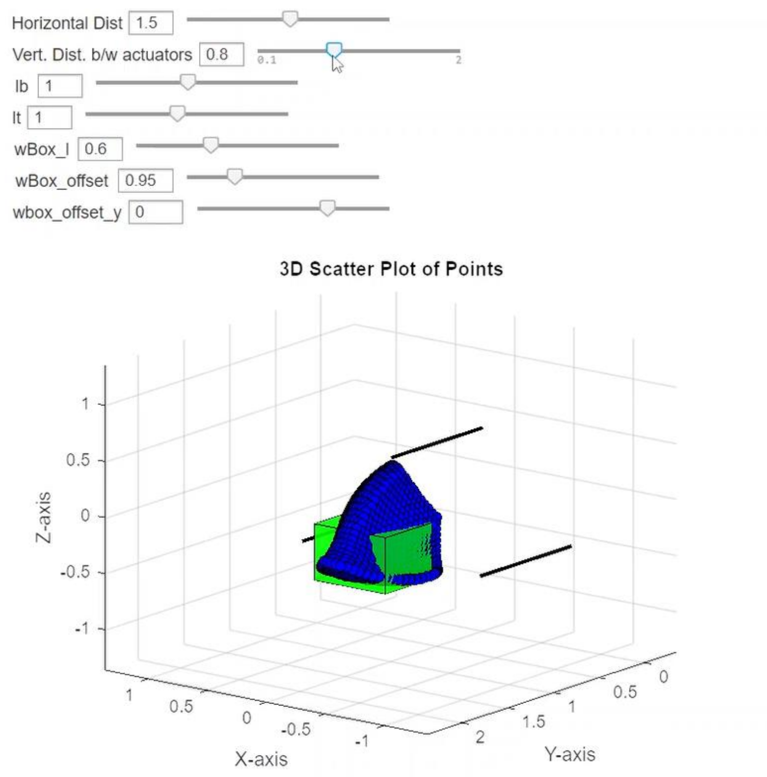

Figure 20: MATLAB Live Script to change the dimensions of the robot

Using this technique, we finalized the following dimensions for our robot:

Table 1: Final Dimensions of outer structure

Horizontal distance between Actuators	1 m
Vertical Distance between actuators	0.7 m
Length of lower Links	1 m
Length of Upper Links	1 m

3.9 Simscape Simulation

After all the equations have been derived and all the dimensions have been finalized, we created a simulation using the Simscape Multibody Module. This model allowed us to define all the joints, dimensions, and links, and its solver allowed us to see how the end-effector would move given a specific input.

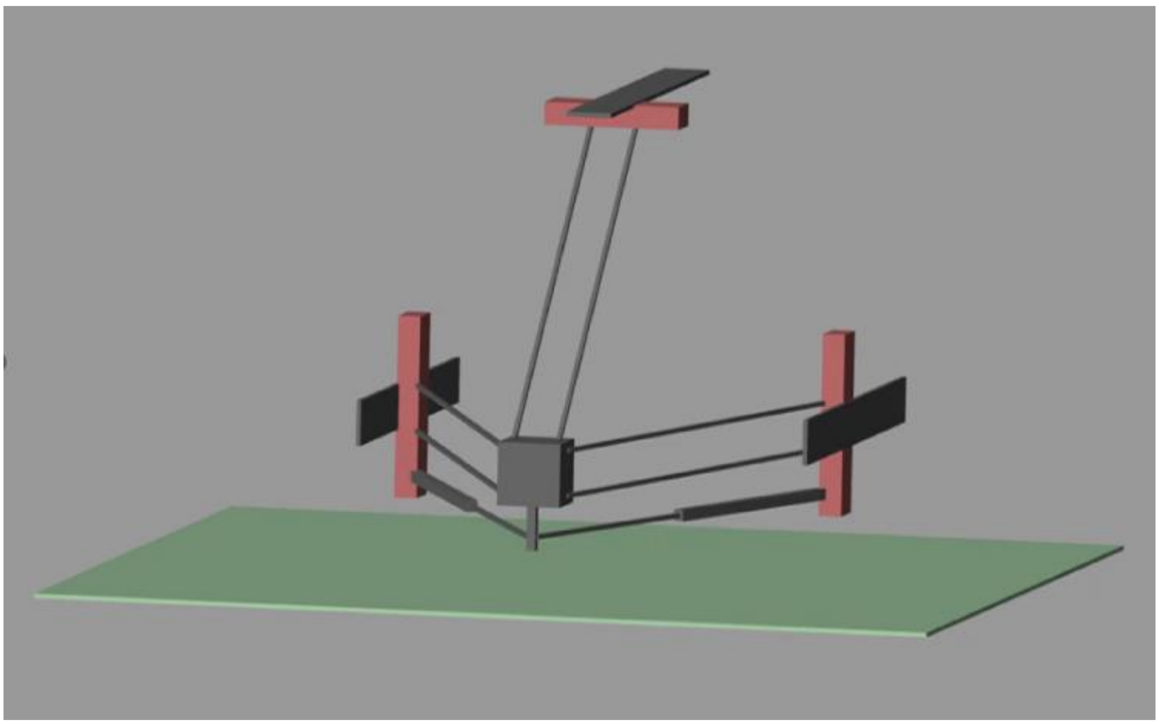

Figure 21: Simscape Multibody Simulation of our Parallel Robot

Furthermore, we created different paths for the end-effector to move in and tested it out on the simulation. This way, instead of testing the trajectories on the real robot, we can first test it on the simulation and find out any errors beforehand.

3.10 Outer Structure

Next step was developing the CAD and figuring out the basic joining mechanisms. Using the dimensions achieved, following structure was modeled on Fusion 360.

Figure 22: CAD of outer structure

It is apparent in the model that the 3 linear actuators, which are considerably heavy, are given sufficient supports so to maintain precise motion of the effector. This was validated using ANSYS Mechanical. Following shows the deflection of the upper aluminum extrusions due to the weight of the linear slide base.

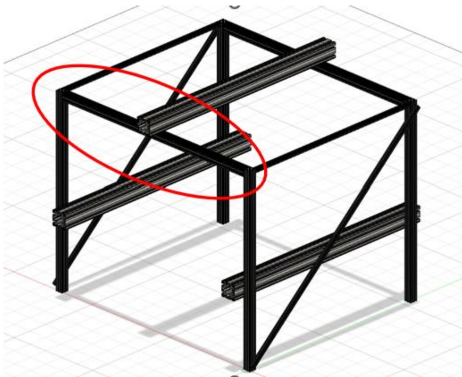

Figure 23: Analyzing the top extrusion

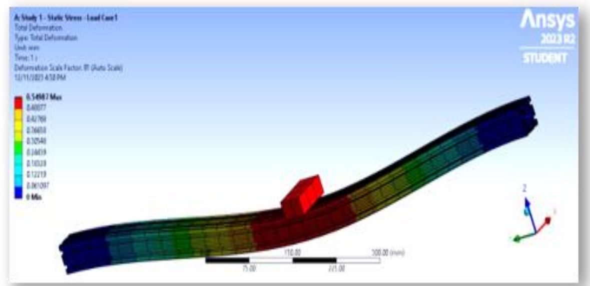

Figure 24: Ansys simulation of top extrusion

Given the weight of the actuator, the extrusion only undergoes deflection of around 0.5mm which is acceptable for the prototype we are developing.

There is one important point to be noted. If in case this was a serial robot, such a small misalignment would have resulted in a quite a large offset at the end effector due to inherent design of serial robots. Here in parallel robot, there is no such problems.

Next, we wanted to study the effects of dynamic forces when the actuators are at maximum acceleration. Applying simply Newton’s Second Law, we found the maximum dynamic load. Following shows the maximum stress under these loading condition.

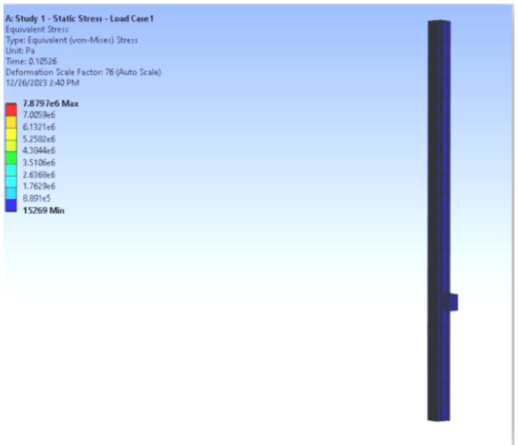

Figure 25: Ansys Simulation of Left Extrusion

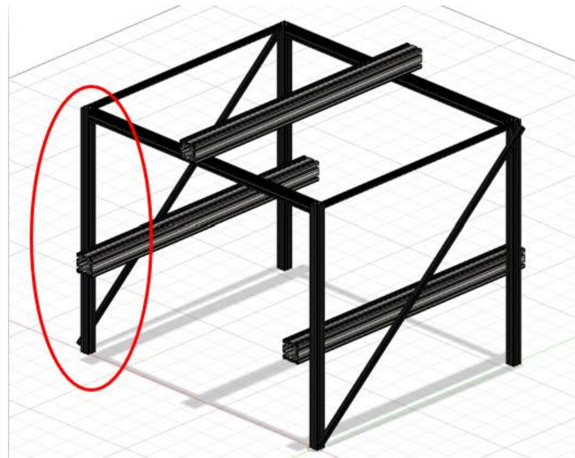

Figure 26: The left extrusion

The stress and lateral deflections under the dynamic loading are minimal and so good to move on with.

The same simulations were carried out for different extrusions sizes and we finalized 40/40 for load bearing i.e. supporting the actuators and all other were 20/20. This ensured reasonable strength and cost effectiveness.

3.11 Clamping Mechanism

The link lengths and the dimensions of the structure were finalized and next was to assemble them through a proper clamping mechanism.

We wanted the mechanism to be modular so that it can be adjusted to any base. This will not limit our design to a particular type of actuator and so provides freedom of modularity in the entire machine.

There were multiple proposed designs for clamping mechanism. Each of those was analyzed under different loading conditions and following was finalized:

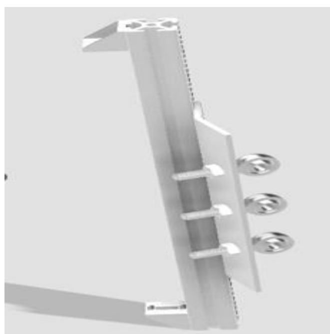

Figure 27: Clamping Mechanism CAD

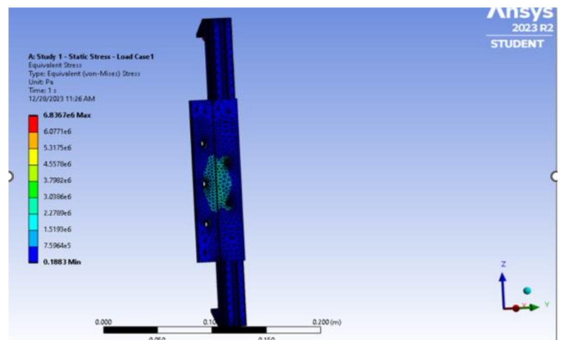

Figure 28: Clamping Mechanism Ansys Simulation

This simple sheet metal design ensures lower moving mass, and modularity. Also, since the end effector will be 3D printed using appropriate polymer so lower mass, thus the deflection induced is very small.

3.12 PHS Rod End Bearings

Next is the most important connection, PHS rod end bearings which connect the linkages to the clamping mechanism. Though our payload was very small, still we wanted to follow the entire procedure as suggested by SKF bearing standards to choose our bearings. This we did since these bearings are one of the most crucial component of our design.

After following the SKF catalog, we were able to figure out that for our payload of 15kg, the minimum bearing was also suitable, which is 4mm bore. However such a small linkage was not easy to find.

Going into the market, we finalized SA6T/K rod end bearing which was locally available. So corresponding shank size for the linkage was achieved to be 6mm as well.

Figure 29: PHS Rod End Bearings

3.13 End Effector

For the end effector, the aim was to design it as simple as possible while fulfilling all our requirements. The main requirements are as follows:

- Be as light as possible
- Hold the Rod End bearings at an angle
- Attach the lower links to the nib (bottom part) at an angle
- Incorporate a universal joint to join the upper body with the nib to allow for two degrees of freedom

Keeping in mind that we want the end effector to be light, aluminum sheets have been used as a material to design the end effector. Aluminum is light weight and can be bent easily. A sheet of thickness 3mm was used and sheared into two pieces for the two parts of the end effector. The upper part is attached to the top three linear actuators and the lower part is linked to the lower two actuators. The two parts of the end effector are linked through the universal joint of stainless steel. A universal joint has two yokes that are connected by a spider. It allows to transmit rotational motions in two directions.

6mm holes were drilled through the universal joint using a carbide drill bit. The two parts of the sheet were bent using the sheet metal bending technique at an angle of 25°. Holes of 6mm and 3mm were drilled in the sheet and then joined together using the screws. Another hole of 3mm was drilled in the lower sheet of the end effector to insert the jubilee clamp for holding the desired objects such as welding torch, drill bit, CNC tools, etc.

The design meeting all the requirements is as follows:

Figure 30: CAD of End Effector

3.14 Custom Software to program the Robot

One of our deliverables was to make the robot easily programmable by a user. To accomplish that, we created a graphical user interface, using python, that allows users to write code in our custom built language, which are then sent to the microcontroller through serial communication, and translated into the robot's motion.

Here are a few commands that can be written within our software:

- **UB**: Bring Upper actuators back to reference position
- **LB:** Bring Lower actuators back to reference position
- **UY-100:** Move the end effector 100 mm in the negative Y direction (i.e. downwards)
- **LR**: Turn the nib to the right
- **LM**: Bring Nib to Middle Position
- **LL:** Bring Nib to Left Position
- **UX+200:** Move the End Effector 200mm in the +X direction.

The software also allows users to save their code and retrieve it later for easy reruns.

Once the 'Run' button is clicked, each line of code is individually sent to the STM32 controller. Once one command has been fully executed, the controller sends back a confirmation message, which then causes the python program to send the next command, until all the code has been executed.

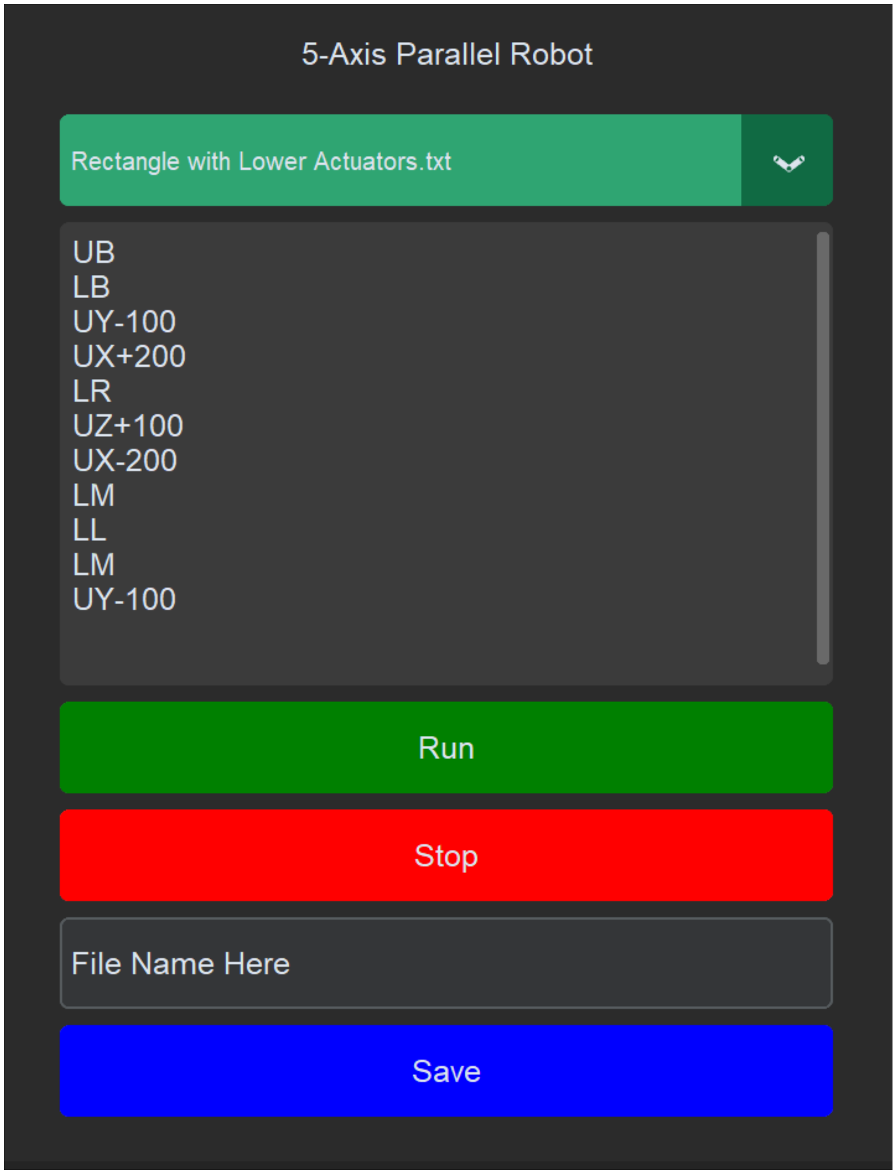

Figure 31: Graphical User Interface developed to allow users to write our custom-built language in order to easily control the motion of the robot.

3.15 Control and Programming

The STM32 was programmed in the C Language. We integrated all the derived forward and inverse kinematic equations into the controller and then used supervisory control to make the actuators move at the right location. To make sure that the actuators follow their instructed paths, we used the P controller. The code was kept modular by creating functions for all important functionalities.

A constant loop of commands gets fed to the STM32 from the serial port, which gets the commands from the python software. The microcontroller determines what actions to take based on the received command through a switch statement.

CHAPTER 4: RESULTS AND DISCUSSIONS

4.1 Overview

Parallel Kinematic Machines (PKMs) represent a cutting-edge innovation in robotics through their ability to be both versatile and precise in various industrial applications. Unlike their serial counterparts, PKMs make use of a parallel structure which enables them to achieve enhanced speeds, accuracy, and payload capacity, making them highly suitable for tasks which require very precise yet complex movement. Hence, PKMs have the ability to attract significant attention from industries including manufacturing, aerospace, automotive, and healthcare etc.

This project explores the design, development, and implementation of a Parallel Kinematic Machine (PKM) capable of operating in a 5-degree-of-freedom (DOF) configuration. By leveraging previous literature, structural analysis, simulations, careful component selection and efficient control system design, the PKM embodies a solution which is only precise and accurate but also highly affordable and easy to assemble.

The primary objective of this project was to design and fabricate a 5 DOF parallel robot which can carry out precise movements and while carrying high payloads within a defined workspace. The second objective is to optimize the robot’s performance by conducting experiments and testing to determine the ideal parameters for the control system. The third objective is to evaluate the capabilities of the robot by commanding it to carry out complex movement maneuvers using measures which include precision, accuracy, and repeatability etc. Another objective is to minimize the overall cost of designing and fabricating to ensure that the robot is economically viable for a country like Pakistan.

4.2 Theoretical Analysis and Simulations

Before moving on to the actual prototype, various theoretical analysis and simulations were carried out to ensure that the robot will not experience any sort of failures when implemented physically. A stress analysis was necessary to ensure that no part of the robot undergoes significant deformation or failure. Since the robot is designed to be precise in its movements, it is important to consider any significant amount of deformation which can be caused by the loadings. A static structural analysis was carried out in ANSYS Mechanical to determine the stresses and deformations in the structure. The results achieved in the actual structure were quite similar to the ones from Ansys.

To accurately simulate the movement of the delta robot, Simscape module from Simulink was used which enabling us to determine the workspace and to cater for any unpredictable movement that the robot could go through during operation.

4.3 Final Structure

The final assembled structure consists of an outer structure made of aluminum extrusions, attached to 5 linear actuators which are connected to the end effector with the help of aluminum rods and clamping mechanisms. Nuts, bolts, and washers are used to create all the fixed joints. This allows for ease in assembly and disassembly of the robot. PHS Rod

End Bearings are used to connect the aluminum rods with the structure and a universal joint is used with the end effector to allow movement in the rotary axes. The circuitry rests on a wooden ply board which can be placed anywhere close to the structure and can also be easily transported. The CAD and the actual prototype of the robot are as follows:

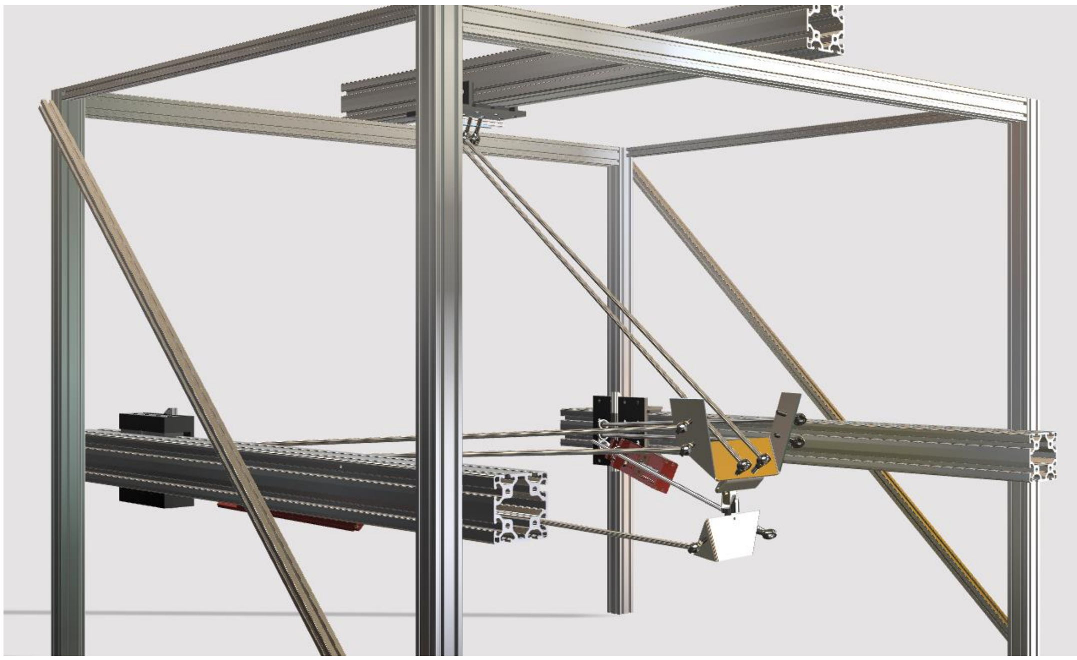

Figure 32: CAD Model (Side View)

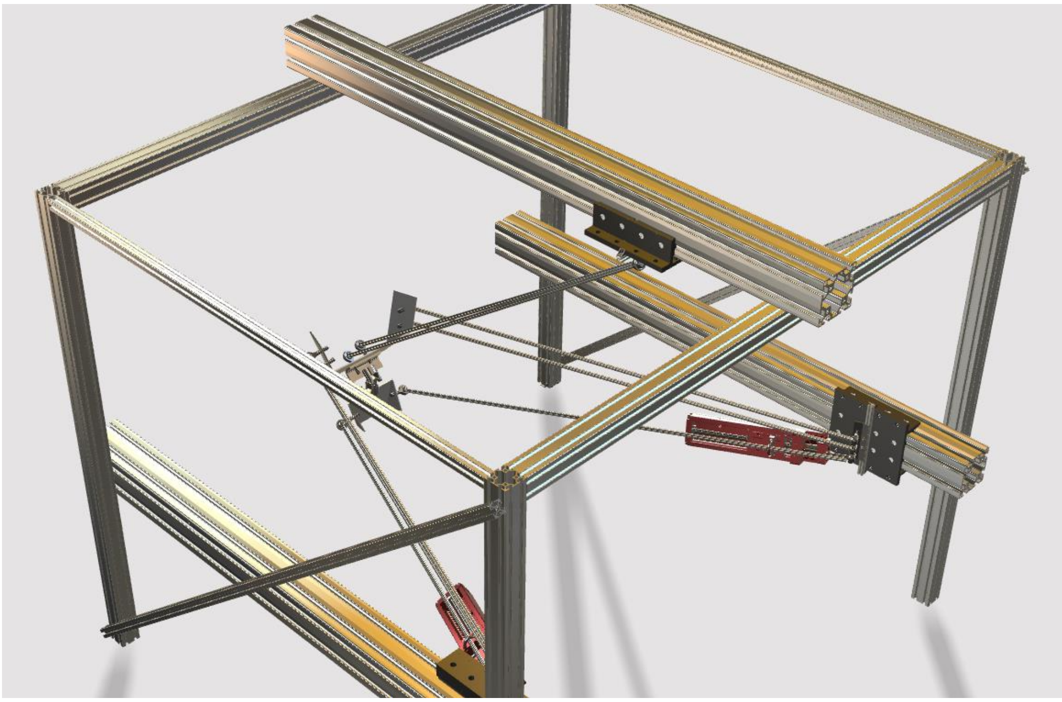

Figure 33: CAD Model (Back View)

Figure 34: Actual Robot (Side View)

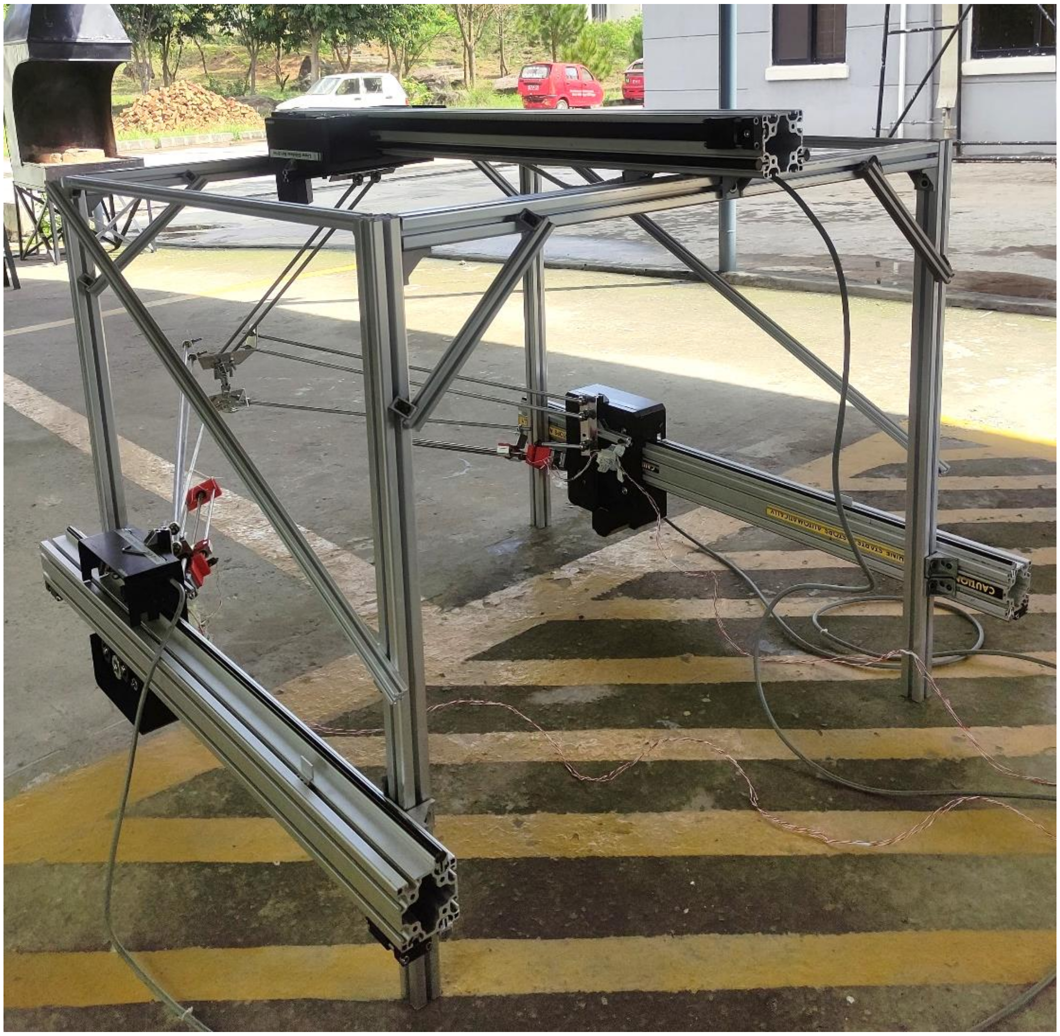

Figure 35: Actual Robot Back View

Figure 36: Front View

4.4 Performance Measures

The robot is tested for different measures to ensure that it performed as per expectations.

The parameters are as follow:

1. Precision
2. Accuracy
3. Repeatability

The results for each of these measures after multiple tests are as follows:

Table 2: Performance parameters of the robot

Measure	Error
Precision	$\pm 5\ mm$
Accuracy	$\pm 2\ cm$
Repeatability	$\pm 5\ mm$

Furthermore, the vibrations were also minimized by the successful tuning of PID parameters used in the control system.

4.5 Summary

Overall, the final structure was as strong and rigid as the one expected from the theoretical analysis. Due to the rigidness of the structure and the precise assembly, dimensional errors and inaccuracies were reduced which has been reflected by the very low vibrations during motion, and the precision in the final positions of the end effector. Furthermore, due to the use of high-quality linear actuators for the 3-dimensional space motion, the load bearing capacity achieved is quite high. Although the accuracy of the robot is good, it still does not meet the industrial standards of today. This can be attributed to some inaccuracies in the final control system, the inaccuracies during assembly of the structure and some inefficiencies in the code.

CHAPTER 5: CONCLUSION AND RECOMMENDATION

In conclusion, parallel robots have the potential to overcome the cons of the more common serial robots. But more importantly, the design and fabrication of a 5-Axis Parallel Robot locally has the potential to uplift the Pakistani manufacturing industry. The accuracy and speed of such a robot can help industries speed up their delivery and improve their quality of products and reduce their reliance on manual labor. Moreover, workers will also be prevented from being involved in potentially dangerous processes such as welding or high speed cutting.

The model that we have developed is the basis of future robots that can be built for specific applications such as welding or cutting. The end effector will need to be redesigned in order to adapt the robot to specific applications.

One of our recommendations to increase the accuracy of the robot is to use stepper motors for the main three linear actuators, instead of brushed DC motors as we have used in our machine. We were limited to the actuators that we had at our disposal, however if someone wishes to rebuild this robot, stepper motors would be a better option for more accurate positioning.

In the future, more research could be done to improve the control algorithm of the robot. Instead of using a PID controller, other control algorithms can be tried and their accuracies can be compared.

REFERENCES

[1] H. Pakistan, "Hyundai AC Assembly Line Pakistan," 2021. [Online]. Available: https://youtu.be/Cp5F0-4k_eg.

[2] I. F. o. Robotics, "China: Robot installations grew by 44 percent," [Online]. Available: https://ifr.org/ifr-press-releases/news/china-robot-installations-grew-by-44-percent.

[3] Cognibotics, "Elha Robotics Automation," [Online]. Available: https://elha-robotic-automation.com/ .

[4] I. F. o. Robotics, "China overtakes USA in robot density," [Online]. Available: https://ifr.org/ifr-press-releases/news/china-overtakes-usa-in-robot-density .

[5] R. A. Systems, "How much do industrial robots cost," [Online]. Available: https://www.roboticautomationsystems.com/blog/how-much-do-industrial-robots-cost/.

[6] J. Merlet, Parallel Robots (Second Edition).

[7] Hindawi, "Motion Reliability Analysis of the Delta Parallel Robot considering Mechanism Errors," *Mathematical Problems in Engineering,* vol. 2019, 2019.

[8] R. W. II, "The Delta Parallel Robot: Kinematics Solutions," January 2016. [Online].

Available: http://www.ohio.edu/people/williar4/html/pdf/DeltaKin.pdf.